Green
Chemistry

Accepted Manuscript

This article can be cited before page numbers have been issued, to do this please use: J. Huang, Q. Hu, X. Guo, Q. Zeng and L. Wang, *Green Chem.*, 2018, DOI: 10.1039/C7GC03744A.

ROYAL SOCIETY
OF CHEMISTRY

rsc.li/green-chem

View Article Online
DOI: 10.1039/C7GC03744A

Green Chemistry

COMMUNICATION

Rethinking $Co(CO_3)_{0.5}(OH)\cdot0.11H_2O$: New property for highly selective electrochemical reduction of carbon dioxide to methanol in aqueous solution

Received 00th January 20xx,
Accepted 00th January 20xx

DOI: 10.1039/x0xx00000x

www.rsc.org/

Jianzhi Huang, Qiong Hu, Xinrong Guo, Qiang Zeng and Lishi Wang*

$Co(CO_3)_{0.5}(OH)\cdot0.11H_2O$ was usually acknowledged and used as a precursor to synthesize other nanomaterials. However, some important properties of $Co(CO_3)_{0.5}(OH)\cdot0.11H_2O$ have not been discovered yet. Herein we report an important new property of hollow urchin-like $Co(CO_3)_{0.5}(OH)\cdot0.11H_2O$ for highly selective electrochemical reduction of carbon dioxide to methanol in $NaHCO_3$ aqueous solution at –0.98 V versus saturated calomel electrode (SCE) with faradic efficiency up to 97.0% under ambient conditions, superior to most of electrocatalysts reported to date. Finally, this low-cost electrocatalyst shows great potential in CO_2 conversion industry for practical application in the future.

Currently, the conversion of carbon dioxide to carbon-containing fuels and chemical products has become research frontier and interesting issue, which can effective reduce the carbon dioxide content and solve the energy crisis.[1,2] And the conversion methods of carbon dioxide to useful products include photochemical,[3] thermochemical,[4] biochemical[5] and electrochemical methods.[6–8] Because of the renewable and clean energy of electricity source and high efficiency of electroreduction, electrochemical reduction of carbon dioxide has become an outstanding pathway toward zero emissions.[9,10] Moreover, electroreduction of carbon dioxide is a convenient method to produce a series of reduced products, such as CO, CH_4, HCOOH, CH_3OH, C_2H_5OH and CH_3COOH, since electroreduction process is composed of multiple electron- and proton-transfer steps.[11,12] Alcohols such as methanol are more desirable among these reduced products, due to its high energy density, easy storage and transportation.[13,14] However, so far, CO_2 reduction has been performed in various electrocatalysts, but the major products for most electrocatalysts are still CO and HCOOH.[1,2] Although CO_2 can be reduced to CH_3OH in thermodynamics at the potential of 0.02 V (versus reversible hydrogen electrode (RHE)).[15–19] Up to now, high selectivity, high faradaic efficiency and low overpotential of methanol formation by electroreduction of carbon dioxide has rarely been reported, due to six electrons participation is difficult to take place in aqueous solution, a more negative potential is required for the formation of methanol.[19,20] Therefore, a low-cost electrocatalyst with good product selectivity, high faradaic efficiency and low overpotential is highly desirable. In Rybchenko's work, pyridine-catalyzed CO_2 electrochemical reduction to methanol was explored on platinum electrodes at high CO_2 pressure (5.5 MPa), with faradaic yield of up to 10%,[21] however, it needs high CO_2 pressure, and also needs noble metal platinum electrodes, all limit its practical use. Quan and co-workers synthesized oxide-derived Cu/carbon catalyst for electroreduction of CO_2 to alcohols, exhibited the faradaic efficiency of 43.2% and 28.0% for methanol and ethanol at –0.94 V (vs. SCE) respectively,[16] however, the product selectivity is low. In Zhang's work, RuO_2/TiO_2 nanotubes composite modified Pt electrode obtained 60.5% faradaic efficiency for methanol at a potential of –0.8 V (vs. SCE),[22] however, this faradaic efficiency was still not enough. In Bocarsly's work, p-GaP semiconductor electrode with a homogeneous pyridinium ion catalyst was used for selective conversion of CO_2 to methanol with light energy, yield faradaic efficiency near 100% with current density of 0.20 mA cm^{-2},[23] but it requires light and uses a complicated catalyst system.

As a non-noble metal, cobalt and its oxides show prominent and promising in CO_2 electrocatalytic reduction recently, especially in Xie's works,[24,25] the partially oxidized Co 4-atom-thick layers attain the highest faradaic efficiency for formate production of 90.1% at –0.85 V (vs. SCE) in 0.1 M Na_2SO_4 solution;[24] the oxygen vacancy-rich Co_3O_4 single-unit-cell layers obtain ca. 85% formate selectivity at –0.87 V (vs. SCE) in 0.1 M $KHCO_3$ aqueous solution.[25] Till now, $Co(CO_3)_{0.5}(OH)\cdot0.11H_2O$ was usually acknowledged and used as a precursor to synthesize other nanomaterials, such as Co_3O_4[25] and CoP.[26] However, some important electrochemical properties of $Co(CO_3)_{0.5}(OH)\cdot0.11H_2O$ have not been discovered yet, the reason may be due to the high

---

Key Laboratory of Fuel Cell Technology of Guangdong Province, School of Chemistry and Chemical Engineering, South China University of Technology, Guangzhou 510641, China
E-mail: wanglsh@scut.edu.cn

Electronic Supplementary Information (ESI) available. DOI: 10.1039/x0xx00000x

View Article Online
DOI: 10.1039/C7GC03744A

performance for CoP and Co_3O_4 respectively used as hydrogen evolution catalyst[26] and supercapacitor,[27] resulting the neglect of electrocatalytic activity of $Co(CO_3)_{0.5}(OH)\cdot 0.11H_2O$ itself, which showed promising in electrochemical reduction of CO_2 to methanol. It is worth mentioning that in latest report,[28] another common $Zn_5(OH)_6(CO_3)_2$ has been proven that exhibits good photocatalytic reduction activity of CO_2 to CO and CH_4 under light irradiation. In this work, we report a new discovery of hollow urchin-like $Co(CO_3)_{0.5}(OH)\cdot 0.11H_2O$ for highly selective electrochemical reduction of carbon dioxide to methanol in aqueous solution, which can realize high selectivity that CO_2 directionally electrochemical reduce to methanol at –0.98 V (vs. SCE) with relative low overpotential of 360 mV in 0.1 M $NaHCO_3$ aqueous solution under ambient conditions, with faradic efficiency of 97.0%, superior to most of electrocatalysts reported to date. Notably, the onset potential for methanol formation is ca. −0.88 V (vs. SCE), corresponding to 260 mV of overpotential, which is a relative low overpotential reported to date for the reduction of CO_2 to methanol. Therefore, the $Co(CO_3)_{0.5}(OH)\cdot 0.11H_2O$ shows great potential in sustainable energy industry in the future.

Schematic of the synthesis of hollow urchin-like $Co(CO_3)_{0.5}(OH)\cdot 0.11H_2O$ through facile hydrothermal method and its application in CO_2 electrochemical reduction was shown in Scheme 1. 62.5 mg cobalt(III) acetylacetonate was added into a solution of 12.5 mL dimethylformamide, 2.5 mL H_2O and 0.625 mL *n*-butylamine. After vigorous stirring for 15 min, the mixture was transferred into a 25-mL Teflon autoclave, heated at 220 °C for 3 h. Finally, the autoclave was cooled down to room temperature, and the product was collected by centrifuging the mixture (washed with cyclohexane and absolute ethanol), then dried in vacuum. The working electrode was fabricated through loading sample suspension onto the glassy carbon electrode. Firstly, 5 mg electrocatalyst was dispersed in 5 mL water and sonicated for 15 min to form a 1 mg mL^{-1} homogeneous suspension. Then, 5 µL of the well dispersed catalyst suspension was loaded onto the pre-polished 3 mm glassy carbon electrode. After drying under infrared lamp, 10 µL of 0.445 wt% Nafion solution (1 mL 5 wt% Nafion solution + 5 mL H_2O + 5 mL absolute ethanol) was dropped onto the surface of the catalyst layer to form a thin protective film, and then dried under infrared lamp. Finally, the well-prepared electrode was used for the CO_2 electrochemical reduction.

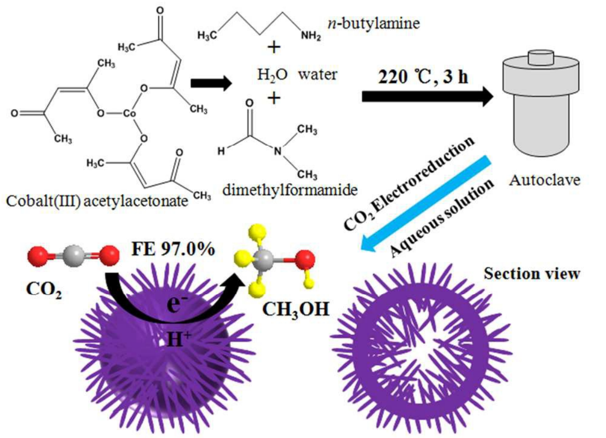

Scheme 1 Schematic of the synthesis of hollow urchin-like $Co(CO_3)_{0.5}(OH)\cdot 0.11H_2O$ and its application in CO_2 electrochemical reduction.

The obtained electrocatalyst was first characterized by X-ray diffraction (XRD), as depicted in Fig. 1A, nice resolved diffraction peaks at 17.1°, 20.3°, 24.4°, 26.6°, 28.4°, 30.4°, 33.7°, 35.0°, 36.4°, 39.3°, 44.3°, 46.8°, 53.7°, 56.0°, 59.3°, 61.9° and 65.4° in XRD pattern can be well indexed to the diffraction from (020), (001), (111), (220), (121), (300), (221), (040), (301), (231), (050), (340), (060), (142), (412), (450) and (023) planes of $Co(CO_3)_{0.5}(OH)\cdot 0.11H_2O$ respectively (JCPDS No. 48-0083), which proves the high purity and good crystallinity of $Co(CO_3)_{0.5}(OH)\cdot 0.11H_2O$. Then, X-ray photoelectron spectra (XPS) measurements were carried out to further investigate the composition and determine the surface electronic state of $Co(CO_3)_{0.5}(OH)\cdot 0.11H_2O$. Only Co, C and O elements can be observed in survey XPS spectrum in Fig. 1B, which also confirmed the formation of pure $Co(CO_3)_{0.5}(OH)\cdot 0.11H_2O$. Moreover, the high-resolution Co 2p spectrum exhibits two prominent peaks at 797.2 and 781.4 eV, corresponding to the Co $2p_{1/2}$ and Co $2p_{3/2}$ spin–orbit peaks[29] of $Co(CO_3)_{0.5}(OH)\cdot 0.11H_2O$ (Fig. 1C). More importantly, two distinct peaks were clearly displayed in high-resolution O 1s core level spectrum in Fig. 1D, according to previous report,[25] one peak at 529.8 eV was deemed as the lattice oxygen, while another peak located at 531.4 eV was ascribed to the oxygen atoms in the vicinity of an oxygen vacancy. Moreover, in Xie's work, these oxygen vacancies have been well studied and proved that can enhance CO_2 electroreduction activity.[25] Therefore, all the above results proved the successful synthesis of high purity and good crystallinity of $Co(CO_3)_{0.5}(OH)\cdot 0.11H_2O$ with distinct oxygen vacancy concentrations.

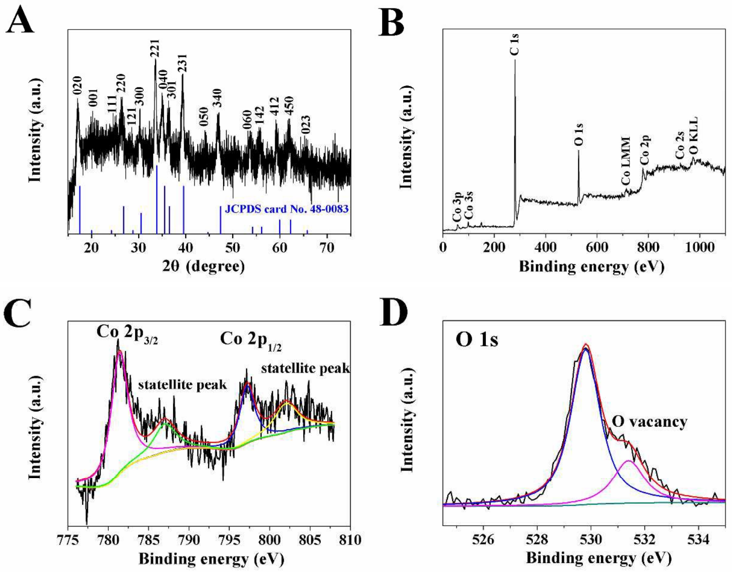

Fig. 1 (A) XRD pattern, (B) survey XPS spectrum, (C) high resolution Co 2p XPS spectrum and (D) high resolution O 1s XPS spectrum of hollow urchin-like $Co(CO_3)_{0.5}(OH)\cdot 0.11H_2O$.

View Article Online
DOI: 10.1039/C7GC03744A

Moreover, the obtained $Co(CO_3)_{0.5}(OH)\cdot0.11H_2O$ electrocatalyst was further studied by scanning electron microscope (SEM) and transmission electron microscopy (TEM). Fig. 2A and 2B depict SEM images at low and high magnification of the obtained $Co(CO_3)_{0.5}(OH)\cdot0.11H_2O$ electrocatalyst with urchin-like morphology in a uniform size of 2 μm. Interestingly, hollow structure was clearly observed in urchin-like $Co(CO_3)_{0.5}(OH)\cdot0.11H_2O$ at low and high magnification TEM images in Fig. 2C and 2D, a thick shell of 300 nm with many nanowires inside and outside on its surface construct the urchin, which significant increased the BET surface area of electrocatalyst and may provide more catalytically surface-active sites for CO_2 reduction. The BET surface area of hollow urchin-like $Co(CO_3)_{0.5}(OH)\cdot0.11H_2O$ electrocatalyst is 52 m^2/g. Moreover, the hollow urchin-like structure of the electrocatalyst was further investigated by STEM image and its corresponding EDS elemental mapping of Co and O elements in Fig. 2E–2H, Co and O elements mainly exists in the shell of the urchin, which also confirmed the hollow structure. Therefore, the unique hollow urchin-like structure and abundant oxygen vacancy of $Co(CO_3)_{0.5}(OH)\cdot0.11H_2O$ made it become a promising electrocatalyst in CO_2 electroreduction.

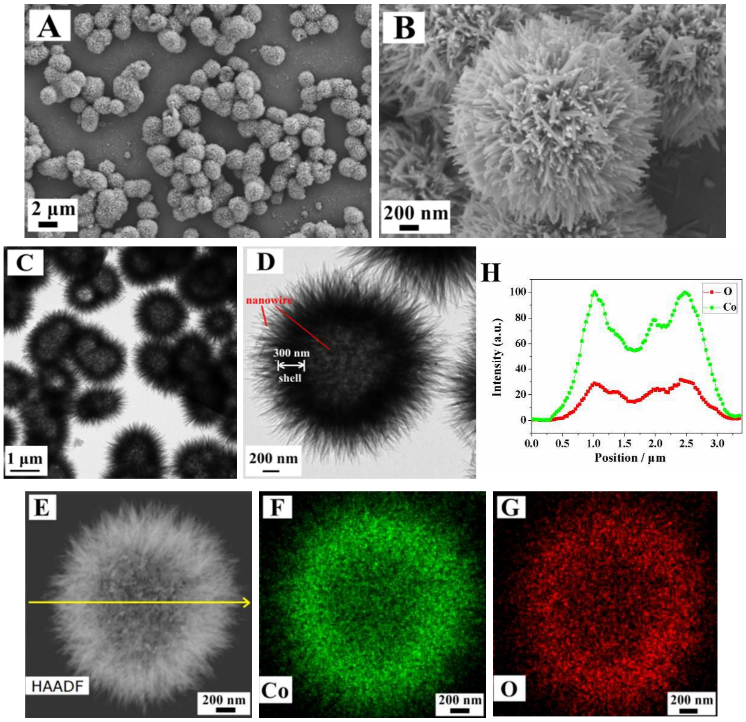

Fig. 2 (A) Low and (B) high magnification SEM images, (C) low and (D) high magnification TEM images of hollow urchin-like $Co(CO_3)_{0.5}(OH)\cdot0.11H_2O$. (E) STEM image, EDS elemental mapping of (F) Co and (G) O, (H) EDS line mapping profile of hollow urchin-like $Co(CO_3)_{0.5}(OH)\cdot0.11H_2O$ along the direction marked by the yellow lines in (E).

With the unique hollow urchin-like structure and abundant oxygen vacancy determined above, hollow urchin-like $Co(CO_3)_{0.5}(OH)\cdot0.11H_2O$ electrocatalyst was applied for CO_2 electroreduction. As depicted in Fig. 3A, linear sweep voltammetry test was first respectively performed in CO_2 or N_2 saturated 0.1 M $NaHCO_3$ aqueous solution. A significant reduction peak was observed for hollow urchin-like $Co(CO_3)_{0.5}(OH)\cdot0.11H_2O$ electrode in CO_2-saturated 0.1 M $NaHCO_3$ aqueous solution (pH=6.7), while no reduction peak appears under N_2 atmosphere, demonstrating that CO_2 can be electrochemically reduced on hollow urchin-like $Co(CO_3)_{0.5}(OH)\cdot0.11H_2O$ electrode. This obvious reduction peak under CO_2 atmosphere can reveal the electroreduction of CO_2, which was also observed for other metal oxide catalysts such as partially oxidized Co, Co_3O_4 and oxide-derived Cu in some previous reports.[16,24,25] CO_2 can be reduced to CH_3OH in thermodynamics at the potential of 0.02 V (vs. RHE), based on following equation: E(vs. SCE) = E(vs. RHE) − 0.059 × pH − 0.241 (V),[15−19] in this system, CO_2 can be reduced to CH_3OH at the potential of −0.62 V (vs. SCE) in aqueous solution (pH=6.7). Notably, in Fig. 3A, the onset potential for methanol formation is ca. −0.88 V (vs. SCE), corresponding to an overpotential of 260 mV, which is a relative low overpotential reported to date for the reduction of CO_2 to methanol. Hollow urchin-like $Co(CO_3)_{0.5}(OH)\cdot0.11H_2O$ electrode generates a biggest current density of 0.59 mA cm^{-2} at −0.98 V (vs. SCE), corresponding to an overpotential of 360 mV. Moreover, constant-potential electrolysis was applied at −0.98 V (vs. SCE) for 10 h in 0.1 M $NaHCO_3$ aqueous solution with CO_2 flow, and the liquid products were qualitative and quantified analyzed by ^1H and ^{13}C nuclear magnetic resonance (NMR). As shown in Fig. 3B and 3C, significant peaks at 3.32 ppm and 49.1 ppm were respectively observed at ^1H-NMR (Fig. 3B) and ^{13}C-NMR spectra (Fig. 3C), attributed to methanol (DMSO is used as an internal standard at ^1H-NMR spectra for quantification of methanol). Moreover, no other liquid products were observed, the results revealed that hollow urchin-like $Co(CO_3)_{0.5}(OH)\cdot0.11H_2O$ electrocatalyst exhibits excellent selectivity for electroreduction of CO_2 to methanol under ambient conditions. CO_2 molecules were directionally converted to methanol with high selectivity, and attained 97.0% faradic efficiency (2.0% faradic efficiency of H_2 and 0.7% of CO were detected by GC). To the best of our knowledge, without injecting external H_2 to hydrogenation, without solar light irradiation, without high pressure or high temperature, such high faradaic efficiency has never been reported to date. The hollow urchin-like structure of electrocatalyst minimized the diffusion resistance for mass transfer, contributing to the efficient transfer of CO_2 and diffusion of the methanol product,[16] and the oxygen vacancies in electrocatalyst also enhance CO_2 electroreduction activity.[25] Moreover, in order to better confirm the advantage of hollow urchin-like structure of the electrocatalyst, a reference electrocatalytic material was being compared. We have prepared solid flower-like $Co(CO_3)_{0.5}(OH)\cdot0.11H_2O$, its SEM image, TEM image, XRD pattern, linear sweep voltammogram and faradaic efficiency were shown in Fig. S1 (Electronic Supplementary Information). Compared with solid flower-like $Co(CO_3)_{0.5}(OH)\cdot0.11H_2O$, much stronger CO_2 reduction peak was observed at linear sweep voltammogram of hollow urchin-like $Co(CO_3)_{0.5}(OH)\cdot0.11H_2O$. In addition, the methanol faradaic efficiency of hollow urchin-like $Co(CO_3)_{0.5}(OH)\cdot0.11H_2O$ (97.0%) was much higher than solid flower-like $Co(CO_3)_{0.5}(OH)\cdot0.11H_2O$ (49.5%). These results showed that hollow urchin-like structure of the catalyst can improve the catalytic reduction activity of CO_2. In contrast with the formate product obtained from partially oxidized

View Article Online
DOI: 10.1039/C7GC03744A

Co 4-atom-thick layers catalyst[24] or oxygen vacancy-rich Co_3O_4 single-unit-cell layers catalyst[25] in Xie's works, the electroreduction product of hollow urchin-like $Co(CO_3)_{0.5}(OH)\cdot 0.11H_2O$ electrocatalyst was methanol. Moreover, we have synthesized Co sphere (Fig. S2) and hollow urchin-like Co_3O_4 (Fig. S3), the electrochemical tests were performed in the same conditions. Compared with the onset potential of the CO_2 electroreduction on hollow urchin-like $Co(CO_3)_{0.5}(OH)\cdot 0.11H_2O$ (−0.88 V (vs. SCE)), the onset potential of the CO_2 electroreduction on hollow urchin-like Co_3O_4 was observed at more negative value (−1.00 V (vs. SCE)). The results showed the only liquid product for Co sphere and hollow urchin-like Co_3O_4 was formic acid, according with the results of previous reports.[24,25] However, the hollow urchin-like $Co(CO_3)_{0.5}(OH)\cdot 0.11H_2O$ was first applied for CO_2 electroreduction in this work, the only liquid product was methanol. The valence of cobalt atom for these materials: Co(0), Co_3O_4(+8/3), $Co(CO_3)_{0.5}(OH)\cdot 0.11H_2O$(+2). We assumed that the valence of cobalt atom may determine the liquid product. The valance of 0 and +8/3 may favour the formation of formic acid, but +2 may favour the formation of methanol. As one of the best metals to obtain methanol, Cu electrode (3 mm in diameter) was also applied for CO_2 electrochemical reduction,[30] the electrochemical test was performed in the same condition. The result showed the Cu electrode can obtain the liquid product of methanol same as hollow urchin-like $Co(CO_3)_{0.5}(OH)\cdot 0.11H_2O$ (Fig. S4). The effect of bare glassy carbon electrode substrate can be neglected, which showed inert for electrocatalytic CO_2 reduction in linear sweep voltammogram, and no signal of methanol can be detected at ^{1}H-NMR spectra (Fig. S5). In addition, the effect of Nafion film can be neglected, there was not obvious CO_2 reduction behaviour of bare glassy carbon electrode with Nafion film in its linear sweep voltammogram, and no methanol product can be detected (Fig. S6). In order to further verify methanol derived from CO_2 electroreduction, control experiment was performed on hollow urchin-like $Co(CO_3)_{0.5}(OH)\cdot 0.11H_2O$ electrocatalyst in N_2-saturated 0.1 M $NaHCO_3$ aqueous solution at −0.98 V (vs. SCE) for 10 h, no methanol was detected at ^{1}H-NMR spectra in Fig. S7, confirmed that methanol was synthesized from CO_2 electroreduction.

The performance of the hollow urchin-like $Co(CO_3)_{0.5}(OH)\cdot 0.11H_2O$ electrocatalyst for electrocatalytic CO_2 reduction under various potentials was further investigated by constant-potential electrolysis. Fig. 3D and Fig. S8A respectively present average production rates for methanol normalized by catalyst loading and available reaction area under various electrolysis potentials, which obtained from the data of electroreduction of CO_2 for 10 h. The production rates of methanol increased with the increasing of applied potential from −0.88 to −0.98 V (vs. SCE), and respectively attained maximum production rates of 145.0 mmol g^{-1} h^{-1} and 3.30 μmol cm^{-2} h^{-1} methanol at −0.98 V (vs. SCE). Production rates of methanol almost keep constant with the increasing of electrolysis potential from −0.98 to −1.10 V (vs. SCE). However, the production rate for methanol normalized by charge (Fig. S8B) increased with the increasing of applied potential from −0.88 to −0.98 V (vs. SCE), and attained maximum production rate of 0.168 μmol C^{-1} h^{-1} methanol at −0.98 V (vs. SCE), then declined with the increasing of electrolysis potential from −0.98 to −1.10 V (vs. SCE). Linear sweep voltammograms of different catalyst loadings were shown in Fig. S9, the biggest CO_2 reduction peak was observed at 5 μL of 1 mg mL^{-1} hollow urchin-like $Co(CO_3)_{0.5}(OH)\cdot 0.11H_2O$. Thus, 5 μL catalyst suspension was chosen as the best catalyst loading in this work. Notwithstanding the high faradaic efficiency to methanol, both actual current density and methanol production rate are very low. Thus, nearly no variation of the pH during time on reaction can be observed. The faradic efficiency for producing methanol, carbon monoxide and hydrogen at various electrolysis potentials was shown in Fig. 3E, the faradic efficiency for methanol increases initially (−0.88 to −0.98 V (vs. SCE)), reaching the maximum of 97.0% at −0.98 V (vs. SCE) with 2.0% of H_2 and 0.7% of CO. However, with the electrolysis potential shifted to more negative value, the faradaic efficiency for methanol production decreases due to the increase in hydrogen evolution reaction (HER) and carbon monoxide formation, which compete with electroreduction of CO_2 to methanol under these conditions. Moreover, CO_2 reduction electrolysis at −0.98 V (vs. SCE) for different electrolysis times was also investigated in Fig. 3F, where the amount of methanol product increased with the increase of electrolysis time. Compared with other reported catalysts in Table S1, the hollow urchin-like $Co(CO_3)_{0.5}(OH)\cdot 0.11H_2O$ electrocatalyst shows superior faradaic efficiency for methanol production with relative low overpotential.

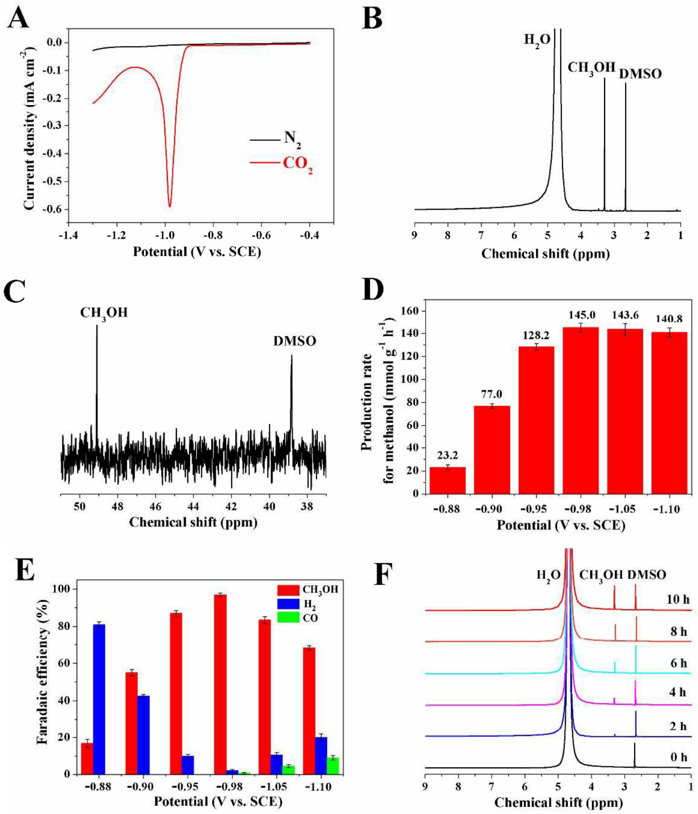

Fig. 3 (A) Linear sweep voltammograms of hollow urchin-like $Co(CO_3)_{0.5}(OH)\cdot 0.11H_2O$ in CO_2-saturated (red line) and N_2-saturated (black line) 0.1 M $NaHCO_3$ aqueous solution (scan rate of 20 mV s^{-1}). (B) ^{1}H-NMR and (C) ^{13}C-NMR spectra of the electrolyte after CO_2 reduction electrolysis at −0.98 V (vs. SCE) for 10 h at the hollow urchin-like $Co(CO_3)_{0.5}(OH)\cdot 0.11H_2O$. DMSO is used as an internal standard at ^{1}H-NMR spectra for quantification of methanol. (D) Production rate of methanol normalized by catalyst loading and (E) Faradaic efficiency

View Article Online
DOI: 10.1039/C7GC03744A

obtained from electrochemical reduction of CO_2 for 10 h at different applied electrolysis potentials. (F) ^{1}H-NMR spectra of the electrolytes after CO_2 reduction electrolysis at −0.98 V (vs. SCE) for different electrolysis times.

During 10 h electrolysis at −0.98 V (vs. SCE) in 0.1 M $NaHCO_3$ aqueous solution with CO_2 flow, the hollow urchin-like $Co(CO_3)_{0.5}(OH)\cdot 0.11H_2O$ electrocatalyst showed negligible decay in current density (0.60 mA cm^{-2}) while maintaining a methanol faradaic efficiency of 97.0% (Fig. S10A), indicating a stable electroreduction process catalyzed by the hollow urchin-like $Co(CO_3)_{0.5}(OH)\cdot 0.11H_2O$ electrocatalyst. After 10 h electrolysis test, the electrocatalyst was characterized by XRD, SEM and TEM. As shown in Fig. S10B, S10C and S10D, XRD pattern of electrocatalyst after test was also well indexed to the diffraction peaks of $Co(CO_3)_{0.5}(OH)\cdot 0.11H_2O$ (JCPDS No. 48-0083), and the hollow urchin-like structure of electrocatalyst was also preserved, which proves the stability of $Co(CO_3)_{0.5}(OH)\cdot 0.11H_2O$ electrocatalyst.

Finally, we further investigated the hollow urchin-like $Co(CO_3)_{0.5}(OH)\cdot 0.11H_2O$ electrocatalyst for CO_2 electroreduction in various aqueous solutions, linear sweep voltammetry test and constant-potential electrolysis were respectively performed in CO_2-saturated 0.1 M NaCl (pH=3.9), 0.1 M Na_2SO_4 (pH=4.3) and 0.1 M $NaNO_3$ (pH=4.1) aqueous solutions. In Fig. 4A, a biggest current density of 0.72 mA cm^{-2} at −1.08 V (vs. SCE) was observed in NaCl aqueous solution, and the onset potential for CO_2 electroreduction was –0.87 V (vs. SCE). A maximum current density of 0.22 mA cm^{-2} at −1.15 V (vs. SCE) and onset potential at −0.88 V (vs. SCE) were observed in Na_2SO_4 aqueous solution in Fig. 4B. In Fig. 4C, a biggest current density of 0.69 mA cm^{-2} at −0.95 V (vs. SCE) and onset potential at −0.80 V (vs. SCE) were observed in $NaNO_3$ aqueous solution. Moreover, ^{1}H-NMR spectra of various electrolytes after CO_2 constant-potential electrolysis at their reduction peak potentials were shown in Fig. 4D, only methanol product can be observed without any other liquid products. And the faradaic efficiency for methanol in NaCl, Na_2SO_4 and $NaNO_3$ aqueous solutions were 94.1%, 84.3%, 92.5% respectively (Fig. 4E). These results showed that CO_2 can be selective electrochemical reduced to methanol with high faradic efficiency in various aqueous solutions at hollow urchin-like $Co(CO_3)_{0.5}(OH)\cdot 0.11H_2O$ electrocatalyst, indicating the effects from various electrolyte anions to such high selectivity were negligible. Based on previous experimental studies as well as density functional theory (DFT) calculations,[16,31–33] the electroreduction process of CO_2 to CH_3OH is composed of multiple electron- and proton-transfer steps. Possible high selectivity reaction mechanism for electrochemical reduction of CO_2 to CH_3OH on hollow urchin-like $Co(CO_3)_{0.5}(OH)\cdot 0.11H_2O$ electrocatalyst in aqueous solution was proposed in Fig. S11. The structural formula of $Co(CO_3)_{0.5}(OH)\cdot 0.11H_2O$ was shown in Fig. S11, the reaction centre site was Co atom. CO_2 was first adsorbed on the catalyst surface, and then was activated by an electron to form the intermediate CO_2^{*-} anion radical, linked by a C-Co bond. Subsequently, the obtained CO_2^{*-} reacts with a proton−electron pair and forms the *COOH intermediate. The *COOH further reacts with another proton−electron pair to form *CO. Then, the *CO was further reduced to CH_3OH. Finally, the CH_3OH product was desorbed from the catalyst surface.

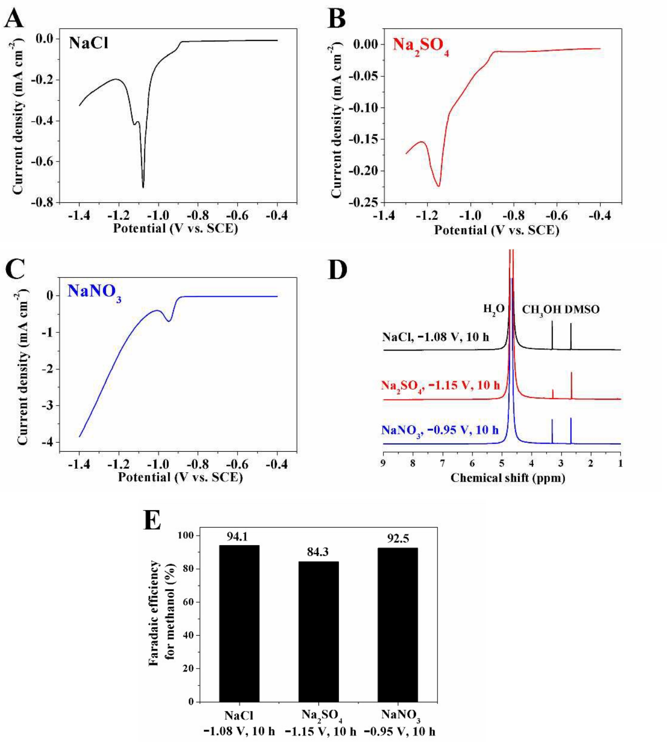

Fig. 4 Linear sweep voltammograms of hollow urchin-like $Co(CO_3)_{0.5}(OH)\cdot 0.11H_2O$ in CO_2-saturated (A) 0.1 M NaCl, (B) 0.1 M Na_2SO_4 and (C) 0.1 M $NaNO_3$ aqueous solution (scan rate of 20 mV s^{-1}). (D) ^{1}H-NMR spectra of 0.1 M various electrolytes after CO_2 reduction electrolysis for 10 h. (E) Faradaic efficiency of methanol obtained from electrochemical reduction of CO_2 for 10 h in 0.1 M various electrolytes.

Conclusions

In summary, an important new property of hollow urchin-like $Co(CO_3)_{0.5}(OH)\cdot 0.11H_2O$ for highly selective electrochemical reduction of carbon dioxide to methanol in aqueous solution was reported in this work. CO_2 directionally electrochemical reduce to methanol at –0.98 V (vs. SCE) with faradic efficiency of 97.0% in 0.1 M $NaHCO_3$ aqueous solution under ambient conditions, with relative low overpotential of 360 mV, superior to most of electrocatalysts reported to date. Moreover, the onset potential for methanol formation is ca. −0.88 V (vs. SCE), corresponding to 260 mV of overpotential, which is a relative low overpotential reported to date for the reduction of CO_2 to methanol. The hollow urchin-like structure of $Co(CO_3)_{0.5}(OH)\cdot 0.11H_2O$ facilitates the transfer and reduction of CO_2 and diffusion of the methanol product, the oxygen vacancies in electrocatalyst also enhance CO_2 electroreduction activity. Finally, this low-cost electrocatalyst was successfully applied in various aqueous solutions for electroreduction of CO_2 to methanol with high faradic efficiency, which will great benefit the development of sustainable energy economy.

Conflicts of interest

View Article Online
DOI: 10.1039/C7GC03744A

There are no conflicts to declare.

Acknowledgements

This work was financially supported by the National Natural Science Foundation of China (Grant Nos. 21475046, 21427809, 21645004).

Notes and references

1 J. Qiao, Y. Liu, F. Hong and J. Zhang, *Chem. Soc. Rev.*, 2014, **43**, 631–675.
2 A. J. Martín, G. O. Larrazábal and J. Pérez-Ramírez, *Green Chem.*, 2015, **17**, 5114–5130.
3 X. Jiao, Z. Chen, X. Li, Y. Sun, S. Gao, W. Yan, C. Wang, Q. Zhang, Y. Lin, Y. Luo and Y. Xie, *J. Am. Chem. Soc.*, 2017, **139**, 7586–7594.
4 S. Kattel, P. Liu and J. G. Chen, *J. Am. Chem. Soc.*, 2017, **139**, 9739–9754.
5 C. Liu, B. C. Colón, Z. Marika, P. A. Silver and D. G. Nocera, *Science*, 2016, **352**, 1210–1213.
6 S. Zhang, P. Kang and T. J. Meyer, *J. Am. Chem. Soc.*, 2014, **136**, 1734–1737.
7 Y. Liu, S. Chen, X. Quan and H. Yu, *J. Am. Chem. Soc.*, 2015, **137**, 11631–11636.
8 Y. Song, W. Chen, C. Zhao, S. Li, W. Wei and Y. Sun, *Angew. Chem. Int. Ed.*, 2017, **56**, 10840–10844.
9 G. Centi, E. A. Quadrelli and S. Perathoner, *Energy Environ. Sci.*, 2013, **6**, 1711–1731.
10 D. R. Kauffman, J. Thakkar, R. Siva, C. Matranga, P. R. Ohodnicki, C. Zeng and R. Jin, *ACS Appl. Mater. Interfaces*, 2015, **7**, 15626–15632.
11 R. J. Lim, M. Xie, M. A. Sk, J. M. Lee, A. Fisher, X. Wang and K. H. Lim, *Catal. Today*, 2014, **233**, 169–180.
12 E. E. Benson, C. P. Kubiak, A. J. Sathrum and J. M. Smieja, *Chem. Soc. Rev.*, 2009, **38**, 89–99.
13 I. Ganesh, *Renewable Sustainable Energy Rev.*, 2014, **31**, 221–257.
14 X. Jiang, N. Koizumi, X. Guo and C. Song, *Appl. Catal., B*, 2015, **170–171**, 173–185.
15 O. A. Baturina, Q. Lu, M. A. Padilla, L. Xin, W. Li, A. Serov, K. Artyushkova, P. Atanassov, F. Xu, A. Epshteyn, T. Brintlinger, M. Schuette and G. E. Collins, *ACS Catal.*, 2014, **4**, 3682–3695.
16 K. Zhao, Y. Liu, X. Quan, S. Chen and H. Yu, *ACS Appl. Mater. Interfaces*, 2017, **9**, 5302–5311.
17 K. P. Kuhl, E. R. Cave, D. N. Abram and T. F. Jaramillo, *Energy Environ. Sci.*, 2012, **5**, 7050–7059.
18 M. Le, M. Ren, Z. Zhang, P. T. Sprunger, R. L. Kurtz and J. C. Flake, *J. Electrochem. Soc.*, 2011, **158**, E45–E49.
19 J. H. Q. Lee, S. J. L. Lauw and R. D. Webster, *Electrochem. Commun.*, 2016, **64**, 69–73.
20 Y. X. Pan, Y. You, S. Xin, Y. Li, G. Fu, Z. Cui, Y. L. Men, F. F. Cao, S. H. Yu and J. B. Goodenough, *J. Am. Chem. Soc.*, 2017, **139**, 4123–4129.
21 S. I. Rybchenko, D. Touhami, J. D. Wadhawan and S. K. Haywood, *ChemSusChem*, 2016, **9**, 1660–1669.
22 J. Qu, X. Zhang, Y. Wang and C. Xie, *Electrochim. Acta*, 2005, **50**, 3576–3580.
23 E. E. Barton, D. M. Rampulla and A. B. Bocarsly, *J. Am. Chem. Soc.*, 2008, **130**, 6342–6344.
24 S. Gao, Y. Lin, X. Jiao, Y. Sun, Q. Luo, W. Zhang, D. Li, J. Yang and Y. Xie, *Nature*, 2016, **529**, 68–71.
25 S. Gao, Z. Sun, W. Liu, X. Jiao, X. Zu, Q. Hu, Y. Sun, T. Yao, W. Zhang, S. Wei and Y. Xie, *Nat. Commun.*, 2017, **8**, 14503–14511.
26 H. Yang, Y. Zhang, F. Hu and Q. Wang, *Nano Lett.*, 2015, **15**, 7616–7620.
27 Y. Wang, A. Pan, Q. Zhu, Z. Nie, Y. Zhang, Y. Tang, S. Liang and G. Cao, *J. Power Sources*, 2014, **272**, 107–112.
28 C. Xin, M. Hu, K. Wang and X. Wang, *Langmuir*, 2017, **33**, 6667–6676.
29 Y. F. Zhao, B. Sun, X. D. Huang, H. Liu ; D. W. Su, K. N. Sun and G. X. Wang, *J. Mater. Chem. A*, 2015, **3**, 5402–5408.
30 C. Genovese, C. Ampelli, S. Perathoner and G. Centi, *Green Chem.*, 2017, **19**, 2406–2415.
31 X. Nie, M. R. Esopi, M. J. Janik and A. Asthagiri, *Angew. Chem. Int. Ed.*, 2013, **52**, 2459–2462.
32 L. Zhang, Z. J. Zhao and J. L. Gong, *Angew. Chem. Int. Ed.*, 2017, **56**, 11326–11353.
33 K. J. P. Schouten, Y. Kwon, C. J. M. van der Ham, Z. Qin and M. T. M. Koper, *Chem. Sci.*, 2011, **2**, 1902–1909.

View Article Online
DOI: 10.1039/C7GC03744A

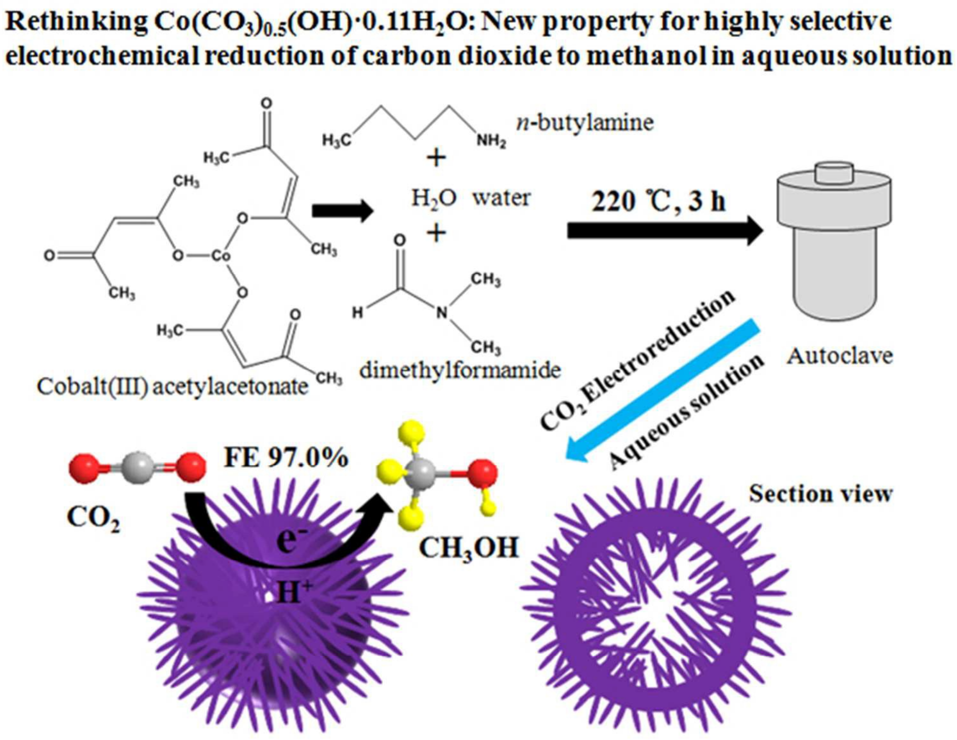

169x128mm (96 x 96 DPI)